Theory and Practice of Science and Technology
2026, VOL. 7, NO. 2, 22-29
DOI: 10.47297/taposatWSP2633-456905.20260702

Remaining Fatigue Life Assessment of Electric Drive Axles Based on Data Augmentation and BiLSTM

Xiuyang Huang

University of Shanghai for Science and Technology, Shanghai, 20093, China

ABSTRACT

The prognosis of remaining fatigue life (RFL) for drive axles is paramount in mechanical engineering; however, the scarcity of empirical fatigue monitoring data, particularly within the electric vehicle (EV) sector, presents a formidable obstacle to accurate durability assessment. This research introduces an innovative two-stage methodology designed for RFL estimation. In the initial phase, a Bidirectional Generative Adversarial Network (BiGAN) is implemented to synthesize degradation trajectories from limited samples and derive corresponding high-dimensional Health Indices (HI). During the subsequent phase, a Bidirectional Long Short-Term Memory (BiLSTM) network is utilized to map multi-channel sensor observations onto these HIs, facilitating regression-based remaining life prediction. Empirical evaluations across diverse drive axle datasets demonstrate robust predictive performance, yielding a mean Root Mean Square Error (RMSE) of 0.0723 and a Mean Absolute Error (MAE) of 0.0375. Furthermore, a 3D-printed drive axle surrogate model was employed to conduct physical bench tests under simulated operating conditions, generating a stress-induced failure dataset. These physical experiments substantiated both the predictive precision and the physical fidelity of the proposed network. The proposed framework significantly bolsters predictive maintenance capabilities within the automotive industry, effectively minimizing downtime, mitigating safety risks, and curtailing operational costs in engineering applications.

KEYWORDS

Remaining fatigue life; BiGAN; BiLSTM; Drive axles

1 Introduction

With the rapid advancements in electric vehicle technology, electric drive axles have garnered significant attention owing to their high efficiency and environmentally sustainable characteristics [1]. However, the fatigue life prediction of electrically driven axles, which face complex loads and working conditions in actual operation, has become a key technology to ensure the safe operation of vehicles. Traditional fatigue life prediction methods include the S-N curve method based on Miner's cumulative damage theory, and other theoretical analysis methods, such as the Corten-Dolon model, have also been used to predict fatigue life [2], [3], [4]. Relying on a large amount of historical data and strict experimental conditions, it is challenging to realize high-precision prediction in the case of data scarcity. Especially in the field of electric drive axles, due to its relatively new technology, full-life data is particularly scarce, which brings significant challenges to fatigue life prediction.

In recent years, significant progress has been made in the application of deep learning techniques to the field of industrial equipment health management, particularly in the area of RFL prediction [5]. Long short-term memory (LSTM) effectively mitigates the gradient vanishing problem encountered by traditional recurrent neural networks (RNNs) when processing time series data, demonstrating powerful representational learning capabilities [6]. In [7], a VMD-based ensemble model that integrates an Echo State Network (ESN) with an optimized LSTM to predict the remaining useful life of lithium-ion batteries, achieving a maximum mean absolute percentage error (MAPE) of just 0.43%. In [8], further validation of the inherent advantages of LSTM in RFL prediction is demonstrated, demonstrating higher accuracy compared to other RNN variants. In [9], an LSTM fusion architecture was proposed that allows for the capture of both local and global features from data collected by multiple sensors. However, conventional LSTM learners are prone to overfitting due to their long-term memory effects. As a result, some researchers have combined LSTM with other networks or analytical models or have made improvements to the LSTM itself. In [10] and [11], LSTM learners are combined with encoders to learn the RFL relationships from time-series sensor data. In [12], a method combining a two-layer temporal convolutional network (TCN) with convolutional self-attention mechanism (CSA) is proposed, which effectively integrates condition monitoring and operating condition data to improve the prediction accuracy of remaining useful life (RUL) across multiple operating conditions. Although these methods have improved prediction accuracy to some extent, the model ' s generalization ability and robustness still require further enhancement in scenarios with scarce data.

Meanwhile, generative adversarial networks (GANs), as a powerful generative model, offer a new approach to addressing the issue of scarce data [13]. In [14], proposes an innovative MEMD-BiGAN risk forecasting method, which enhances the dataset by combining multi-scale analysis and Generative Adversarial Network, thereby improving the reliability of market risk predictions. In [15], a BiGAN-based Risk Generative Adversarial Network model is proposed, which effectively enhances the stability and accuracy of parameter estimation under imbalanced data by incorporating an attention mechanism and an improved discriminator. Additionally, incorporating physical priors and digital twins has emerged as complementary strategies to further address these limitations. For physical prior neural networks, [16] optimizes priors for probabilistic RUL prediction, improving uncertainty handling. Our approach embeds degradation

insights into HI extraction via BiGAN, complementing this. Regarding digital twins, [17] applies them for expert predictive systems. Our data-driven method offers a lightweight alternative for drive axle simulation, validated by 3D-printed experiments, achieving better precision in scarce data settings. Despite these advancements in data-driven RFL prediction meth-ods, the prediction of the lifetime of vehicle-driven axle bridges remains insufficiently studied. This is primarily due to the need for a large amount of high-quality fatigue damage data under multi-axis loading, which involves high data collection costs, complex processes, and the use of multiple sensors and long-term testing. During the structural design phase, lifetime predictions are typically made based on a series of assumptions, but actual loads often differ sig-nificantly from these assumptions. Therefore, accurately pre-dicting using limited service data remains a challenge.

To surmount the aforementioned obstacles, specifically the conundrum of data scarcity in the fatigue life prognosis of electric drive axles, this study articulates a novel two-stage predictive methodology integrating BiGAN and BiLSTM architectures. In contrast to extant paradigms, the proposed approach initially leverages the robust bidirectional mapping capabilities of BiGAN to extract latent degradation features and synthesize a HI. Subsequently, a BiLSTM network is deployed to characterize the long-term dependencies inherent in fatigue accumulation by exploiting its intrinsic forward and backward contextual capture capacities. To authenticate the physical validity of the synthesized data, an innovative physics-based verification scheme is introduced. Through empirical bench tests utilizing a 3D-printed surrogate drive axle model, a stress-induced failure dataset was acquired. This validation substantiated that the generated data meaningfully reflects physical reality rather than mere statistical artifacts. The remainder of this manuscript is organized as follows: Section 2 provides a concise overview of the data acquisition system. Section 3 delineates the theoretical framework and implementation intricacies of the proposed methodology in detail. Section 4 presents the experimental results and comprehensive analysis. Section 5 introduces the complete dataset and outcomes derived from the 3D-printed drive axle experiments. Finally, Section 6 summarizes the proposed approach and outlines potential avenues for future research.

2 Data Acquisition System Design

When the vehicle-driven axle bridge is subjected to external forces, it experiences slight deformations, as shown in Figure 1. Under the action of external pressure on the axle bridge, a deformation displacement *AC'* occurs, and the cross-section generates particular shear stress and shear strain angles, resulting in micro-strain and displacement.

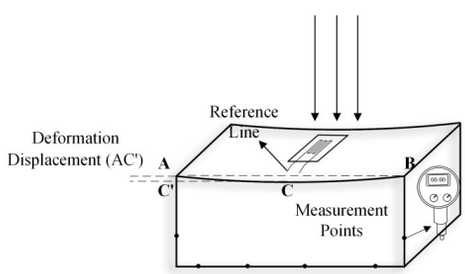

Figure 1 Drive axle deformation diagram

More sensitive strain gauges are used to measure the micro-strain of the vehicle axle, and employ laser range finders or high-precision displacement sensors to continuously monitor the deformation process at the measurement points. As a result, the micro - strain ϵ induced by the applied external force can be obtained as follows:

$$\frac{\Delta R}{R} = K \cdot \epsilon \tag{1}$$

Where there is a change in resistance, R is the initial resistance of the strain gauge, and K is the gauge factor of the strain gauge.

Drawing upon preliminary experimental investigations, a comprehensive data acquisition system was architected to precisely quantify the micro-strains and displacements of the drive axle under authentic operational environments. The apparatus utilizes dual loading motors to exert controllable magnitudes of force upon the drive axle, thereby simulating the stress distribution across diverse operating conditions. The front-end signal acquisition suite comprises twelve strain sensors and eight displacement sensors. Transduced signals from these sensors are processed via bridge boxes, facilitating the conversion of mechanical strain into resistive electrical signals. These analog signals are subsequently filtered and digitized through a data acquisition board before being transmitted to a host computer for systematic logging and analysis. This system ensures the veracity and stability of data collection, thereby providing high-fidelity input for the subsequent fatigue life prognosis models.

3 The Proposed Methodology

3.1 Overarching Framework

This section provides an in-depth elucidation of the proposed drive axle fatigue life prognosis framework, encompassing its structural architecture and procedural workflow. A schematic representation of the articulated methodology is illustrated in Figure 2. Specifically, the blue-contoured region in Figure 2 delineates the collaborative

training mechanism involving the encoder, generator, and discriminator of the BiGAN. This mechanism synthesizes high-fidelity degradation trajectories—spanning from initial loading to ultimate structural failure—derived from constrained multi-channel sensor inputs, while simultaneously extracting HI via the encoding network. The yellow-contoured block characterizes the training phase of the BiLSTM network, which functions to map both empirical and synthesized datasets onto the HI sequence to facilitate regression-based estimation of the remaining fatigue life. Furthermore, the peripheral purple-colored modules describe the comprehensive validation protocols implemented to verify the model's efficacy.

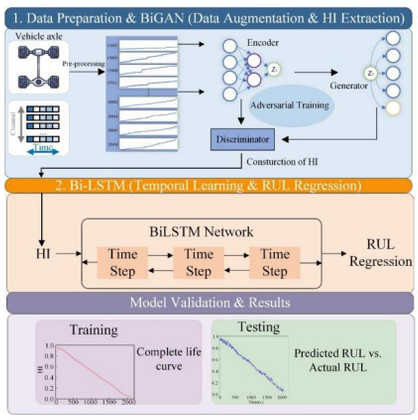

Figure 2 Flowchart of RFL prediction for drive axles

3.2 HI Formulation via the BiGAN Architecture

To synergistically integrate data augmentation with high-order feature dimensionality reduction, this study incorporates an advanced architectural variant termed the BiGAN, as illustrated in Figure 3. In contrast to conventional generative paradigms, BiGAN establishes a closed-loop adversarial ecosystem comprising an encoder, a generator, and a discriminator. The fundamental rationale involves constructing a bidirectional mapping bridge between the physical observation domain and the latent feature space. Specifically, the encoding network facilitates the feature decoupling of multi-source sensor signals and their subsequent compression into a low-dimensional latent space. Concurrently, the generator performs inverse sampling from this latent distribution to synthesize high-fidelity degradation trajectories. Distinct from traditional architectures, the discriminator is no longer restricted to authenticity assessment within a solitary data domain; instead, it evaluates the discrepancies in the joint distribution between empirical and synthetic sample pairs. This mechanism compels the network to synchronously enhance data reconstruction fidelity and the representational efficacy of latent layer features during the adversarial optimization process.

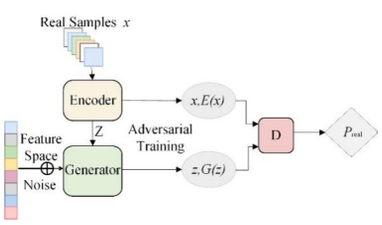

Figure 3 BiGAN architecture diagram

In this study, the input data is assumed to be $X^n = [X^n_1, X^n_2, \cdots, X^n_t]$, where X^n_t represents the sensor reading at time step t. The encoder E maps the input data X^n to the latent space Z, resulting in the latent variable z_t. The generator G samples from the latent space Z to generate data, and the discriminator D distinguishes between the generated data M^n_t and the real data:

$$\begin{aligned} z_t &= E(X^n_t) \\ M^n_t &= G(Z) \\ D(M^n_t, X^n_t) &= P_{\text{real}} \end{aligned} \tag{2}$$

Leveraging the aforementioned closed-loop bidirectional feature projection mechanism, BiGAN demonstrates an inherent topological advantage in surmounting the bottlenecks associated with finite sample datasets, facilitating both the synthesis of degradation trajectories and the high-order extraction of HIs. Within this architectural paradigm, the derivation of the HI is directly traced back to the reconstructive interpretation of latent variables performed by the generative network. Given that the first principal component of the synthesized data M_t typically governs the low-frequency global degradation trend of the system, this intrinsic attribute possesses profound representational significance for modeling fatigue degradation dynamics. Consequently, the first dimension of this sequence is established as the fundamental feature element for HI construction, defined as $HI_t = M_{t,1}$. To eliminate discrepancies in physical dimensions and enforce alignment with the monotonic degradation laws characteristic of the early-to-mid service phases,

a linear min-max normalization mapping, constrained within the interval [0,1], is further applied to the preliminary feature HI_t:

$$HI_t = \frac{M_{t,1} - M_{min}}{M_{max} - M_{min}} \tag{3}$$

Where *Mmin* and *Mmax* represent the minimum and maximum values of the first dimension of the latent variables across all time steps. The final output of the first stage is the HI sequence *{HI1, HI2, ⋯, HIT}*, which serves as the foundation for predictions in the second stage.

3.3 RFL Estimation via the BiLSTM Architecture

Subsequent to the successful isolation of a purified HI that characterizes global degradation through the BiGAN framework, the primary challenge for the prognosis framework shifts toward the precise decoding of the profound fatigue accumulation evolution patterns inherent in multi-source sensor monitoring sequences across the temporal dimension. To resolve this intricate long-range temporal mapping conundrum, a BiLSTM network is integrated to perform end-to-end nonlinear regression analysis directly on sensor-based time-window sequences. The overall systemic workflow is illustrated in Figure 5. By designating the raw multi-sensor data sequences from the training set as input variables and the HI sequences formulated in the initial stage as supervisory labels, a predictive model is trained to facilitate the regression of the remaining fatigue life.

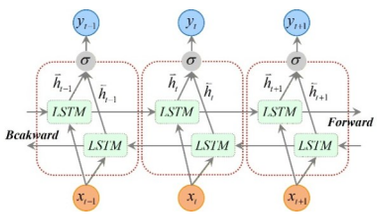

Figure 4 BiLSTM architecture diagram

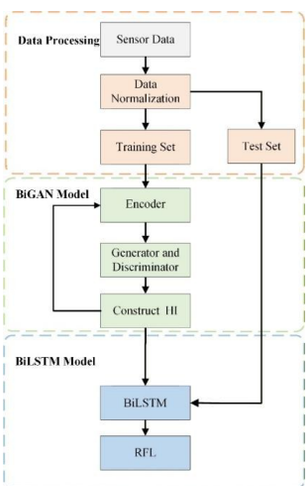

Figure 5 Proposed model of RFL prediction

From the perspective of the physical essence of temporal dynamics, the inception and propagation of fatigue cracks within a drive axle are by no means transient or isolated events; rather, they constitute a continuous degradation process that spans the entire lifecycle. This implies that the degradation state of the equipment at any specific juncture is not merely the inexorable outcome of historical fatigue damage accumulation, but also encapsulates critical precursors that dictate future failure evolution trajectories. Conventional unidirectional RNN or LSTM architectures, constrained by their unidirectional information flow inference mechanisms, are restricted to the passive extraction of historical observations. Consequently, when addressing life prognosis tasks characterized by robust bidirectional correlations, such models are highly susceptible to the discontinuity and loss of contextual degradation features.

To surmount these topological constraints, the BiLSTM network represents an architectural augmentation of the standard LSTM framework. As illustrated in the schematic diagram in Figure 4, it is evident from the underlying structural principle that BiLSTM is not a mere linear stacking of single dimensions. Instead, it is spatially coupled by two parallel, parameter-independent LSTM hidden layers with opposing information flow directions. Within the information transmission mechanism of the network, when a multi-channel sensor data window is fed into the model, the input tensor is simultaneously distributed along two independent pathways: the forward LSTM layer processes data frame-by-frame in strict chronological order from 1 to T, focusing on extracting the forward historical memory of fatigue damage; concurrently, the backward LSTM layer scans the same observation sequence in reverse chronological order from T to 1. This backward recursive scanning aims to leverage future state distributions to retrospectively infer and calibrate the

feature saliency of the current moment.

By virtue of this sophisticated bidirectional scanning mechanism, the BiLSTM architecture facilitates comprehensive contextual modeling of the bidirectional dependencies inherent in the drive axle ' s degradation.

$$\begin{aligned}\vec{h}_t &= \mathrm{LSTM}(f_t, \vec{h}_{t-1}) \\ \overleftarrow{h}_t &= \mathrm{LSTM}(f_t, \overleftarrow{h}_{t+1})\end{aligned} \tag{4}$$

4 Experimental Results and Analysis

4.1 Data Characterization and Preprocessing

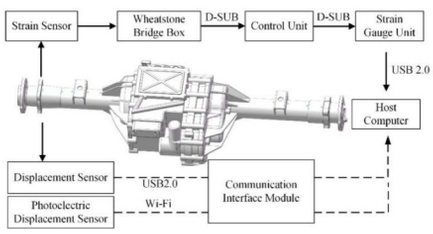

Figure 6 Vehicle axle stress acquisition platform

To evaluate the fatigue life of vehicle drive axles under diverse loading conditions, a specialized experimental apparatus was developed (Figure 6). Five sets of drive axle tests were conducted, with each specimen subjected to eight cycles of repeated pressurization. Data were acquired at a sampling frequency of 100 Hz, yielding approximately 80,366 temporal observations across the multi-channel sensor suite. Prior to analysis, all raw data underwent rigorous calibration and filtering to mitigate noise interference and harmonize disparate physical dimensions. For instance, the historical sensor trajectory is defined as $X = [X_1, X_2, \cdots, X_t]$, where X_t represents the readings from 22 sensors at time step t. Subsequently, channel-wise normalization was implemented to ensure measurement precision and consistency:

$$X_{t,i}^{n} = \frac{X_{t,i} - X_{min,i}}{X_{max,i} - X_{min,i}} \tag{5}$$

4.2 Model Training

Utilizing the preprocessed datasets, the BiGAN architecture employs its encoding network to project raw observations into a latent manifold. Subsequently, the generator synthesizes HI from this latent space, while the discriminator rigorously ensures high-fidelity alignment between the synthetic and empirical HI distributions. To mitigate overfitting, an early stopping strategy is integrated into the adversarial optimization process. Post-training, the extracted HIs are subjected to min-max normalization to constrain values within the [0,1] interval. Following the HI extraction, the BiLSTM prognosis model is implemented. Temporal training samples are constructed via data partitioning and sliding window sampling of the raw multi-channel sensor sequences, with the BiGAN-generated HI curves serving as supervisory ground-truth labels. To facilitate error convergence, a learning rate attenuation strategy is deployed, specifically reducing the rate to one-tenth of its initial magnitude at the training midpoint.The core hyperparameter configurations, refined through a grid search mechanism informed by domain-specific prior knowledge of fatigue signals, are detailed in Table 1. The Adam optimizer was selected to handle adaptive gradient updates in high-noise environments. A hybrid ReLU-Tanh activation scheme was adopted to leverage the linear characteristics of ReLU in negative regions, thereby enhancing model sensitivity to subtle strain fluctuations. To compensate for reduced feature extraction depth, the batch size was set to 64, with learning rates for BiGAN and BiLSTM precisely tuned to 0.0003 and 0.0015, respectively. Training iterations were established at 400 epochs for BiGAN and 300 for BiLSTM, complemented by a step decay technique that reduces the learning rate by 20% every 50 epochs. This comprehensive approach effectively circumvents overfitting risks while ensuring the physical reliability of the RFL estimations.

Table 1 Model Parameter Settings

Parameter	Algorithm	
	BIGAN	BILSTM
Optimizer	Adam	Adam
Activation	ReLU	Tanh
Batch Size	64	64
Learning Rate	0.0003	0.0015
Epochs	400	300

To comprehensively evaluate the performance of the proposed model, several ordinary regression evaluation metrics were used. MSE is used to measure the difference between predicted and actual values. A smaller MSE value indicates a more accurate model prediction. MAE measures the absolute error between predicted and actual values. The calculation formulas are as follows:

$$RMSE = \sqrt{\frac{1}{N}\sum_{i=1}^{N}(y_i - \hat{y}_i)^2}$$
$$MAE = \frac{1}{N}\sum_{i=1}^{N}|y_i - \hat{y}_i| \tag{6}$$

Where y_i is the actual value, y_i is the predicted value, and N is the number of samples. These two evaluation metrics reflect the model's performance and prediction error on the training and test sets.

4.3 Analysis of Experimental Results

The training performance of the proposed model is illustrated in Figure 7. The graphical representation reveals a high degree of concordance between the predicted outcomes and the HI trajectories within the training dataset. To substantiate the robustness and generalization capabilities of the architecture, further empirical validations were executed across datasets derived from multiple other drive axles. As depicted in Figure7, the model consistently captures the evolutionary dynamics of the HI across diverse drive axle specimens with significant precision.

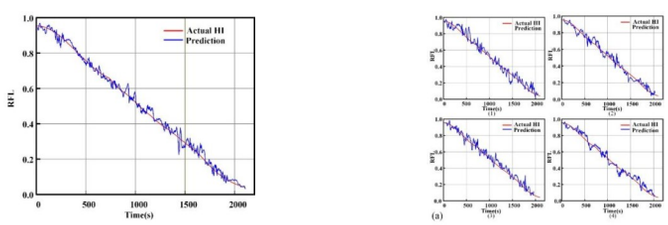

Figure 7 RFL Prediction Chart

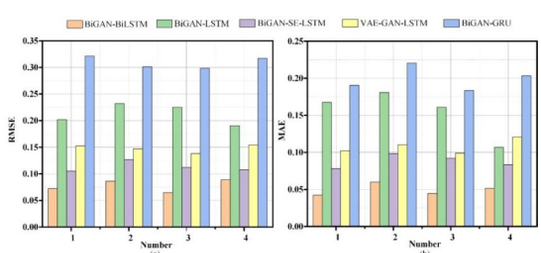

Figure 8 RFL Prediction Chart

To further quantify the superiority of the proposed framework, a comparative analysis was conducted against four mainstream data-driven time-series forecasting methodologies. These baseline paradigms exhibit distinct emphases regarding memory duration and data-processing mechanisms. Furthermore, the hyperparameters for these networks—including iteration epochs, hidden layer depth, and time-delay increments—were subjected to rigorous iterative fine-tuning and optimization. As illustrated by the evaluation metrics in Figure 8 and Table 2, it is empirically evident that the proposed BiGAN-BiLSTM model significantly outperforms the alternative architectures across all assessment criteria. To dissect component contributions, ablation studies were conducted. Substituting the BiLSTM architecture with a conventional unidirectional LSTM significantly escalated prediction error, validating the necessity of bidirectional modeling for integrating dual-path temporal information. The results substantiate a strong synergy: BiGAN provides a compact latent-space health representation, while BiLSTM decodes long-range dependencies. Performance attenuation upon removing either module proves both are indispensable for maximizing prognostic capability, underscoring the framework's structural integrity and engineering efficacy. For statistical validation, five independent trials yielded an average maximum error of 3.8% with a standard deviation of 0.29%. A 95% confidence interval of [3.44%, 4.16%] was derived, confirming that the overall error remains robustly under the 5% threshold at a 95% confidence level.

Table 2 Result of Different Methods

Evaluation index	Algorithm	Average
RMSE	BiGAN-BiLSTM	0.0423
	BiGAN-LSTM	0.2576
	BiGAN-SE-LSTM	0.1022
	VAE-GAN-LSTM	0.1256
	BiGAN-GRU	0.3145
MAE	BiGAN-BiLSTM	0.0582
	BiGAN-LSTM	0.1269
	BiGAN-SE-LSTM	0.0758
	VAE-GAN-LSTM	0.0998
	BiGAN-GRU	0.1958

5 Model Validation and Enhancement

To further evaluate the generalization capabilities of the prognostic algorithm within intricate service environments, a high-fidelity geometric reconstruction of the vehicle drive axle was executed utilizing SolidWorks. Acknowledging the constraints of additive manufacturing, strategic topological simplifications were applied to the hub interfaces and internal reinforcements of the axle housing, while preserving essential structural mechanical characteristics. Regarding material selection, the fatigue properties of aluminum alloy and high-strength 40Cr alloy structural steel were comparatively assessed. Due to its superior hardenability and robust mechanical profile, 40Cr was designated as the additive manufacturing substrate to accurately replicate the stress behavior of the drive axle shaft. Comparative empirical analyses demonstrated that this physical surrogate exhibits exceptional alignment with full-scale components regarding fatigue fracture toughness and crack propagation rates, with error margins consistently remaining within an 8% threshold. The comprehensive experimental testbed is depicted in Figure 9. The surrogate model features a total length of 40 cm, corresponding to a geometric scaling factor of 1:5 relative to the prototype axle. Governed by the principles of mechanical similitude, the experimental loading was derived by scaling the square of the length ratio; consequently, the test load applied to the surrogate was precisely calibrated to 0.04 times the actual service load.

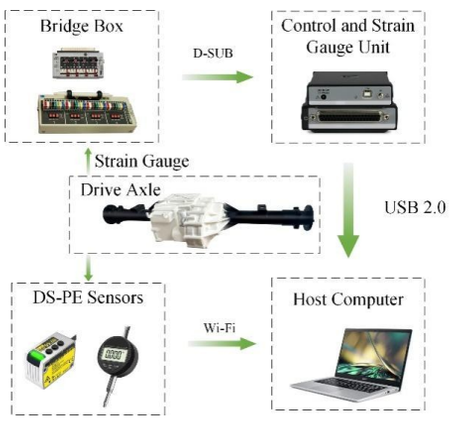

Figure 9 3D Printing Platform

The experimental configuration maintains consistency with Section 3. The data processing workflow strictly adheres to the HI formulation protocols detailed in Section 2 and the RFL estimation methodology described in Section 3. Processed multi-channel features are mapped onto the HI sequence and subsequently integrated into the pre-trained BiGAN-BiLSTM architecture to predict the RFL of the physical surrogate. As illustrated in Figure 10, the empirically derived HI evolution trajectories demonstrate a high degree of concordance with the network's predictive outputs. Critical characteristics—including inflection points and gradient slopes across the nascent, intermediate, and near-failure degradation phases—exhibit significant overlap, with the maximum discrepancy constrained within 5%. Furthermore, several baseline paradigms were evaluated using the identical physical dataset, as depicted in Figure 10. Horizontal comparisons indicate that the proposed prognostic framework outperforms alternative methodologies across all assessment criteria. These findings not only substantiate the validity of the synthesized data from a physical experimental perspective but also affirm the superior robustness and predictive precision of the framework under data-constrained scenarios.

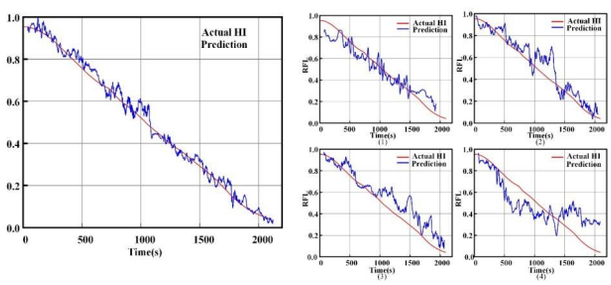

Figure 10 RFL Prediction Chart

6 Conclusion

To address the paucity of full-lifecycle degradation data in the RFL prognosis of vehicle drive axles, this study articulates a dual-phase assessment framework integrating BiGAN and BiLSTM. The initial phase leverages BiGAN for collaborative adversarial training to synthesize high-fidelity degradation samples while extracting HI. Subsequently, the BiLSTM network is deployed to map multi-channel sensor signals onto HI sequences, facilitating end-to-end RFL estimation. Empirical results demonstrate that the proposed architecture significantly outperforms existing mainstream

baseline models. Furthermore, ablation investigations substantiate the indispensability of the core components, as any modification leads to a marked decline in predictive accuracy, thereby validating the structural rationale of the two-stage design. To evaluate engineering utility, accelerated fatigue tests were conducted on an additive-manufactured physical surrogate of the drive axle. The resulting degradation patterns exhibited exceptional alignment with authentic historical data, proving the algorithm's capability to capture physical fatigue evolution even under constrained a priori knowledge. Nevertheless, certain limitations persist for practical deployment, such as the reliance on sophisticated sensor suites and experimental bench data, which inevitably extends calibration cycles. Future on-board applications must address uncertainties including intermittent sensor failure and escalated environmental noise in complex road conditions. Expanding this data-driven architecture to broader automotive components for high-frequency, real-time fatigue warning represents a high-value trajectory for future research. Overall, the BiGAN-BiLSTM framework demonstrates superior performance in data-sparse scenarios, while the cross-disciplinary validation via 3D printing provides robust support for its implementation in enhancing predictive maintenance and system reliability.

References

[1] D. Ronanki, S. A. Singh, and S. S. Williamson, "Comprehensive Topological Overview of Rolling Stock Architectures and Recent Trends in Electric Railway Traction Systems," IEEE Transactions on Transportation Electrification, vol. 3, no. 3, pp. 724-738, 2017.

[2] Y. Chen, W. Men, Z. Yuan et al., "Nonlinear Damage Accumulation Rule for Solder Life Prediction Under Combined Temperature Profile With Varying Amplitude," IEEE Transactions on Components, Packaging and Manufacturing Technology, vol. 9, no. 1, pp. 39-50, 2019.

[3] J. Zhang, Y. Yan, S. Jin et al., "Fatigue tests and design of welded hollow spherical joints in grid structures," Structures, vol. 65, pp. 106590, 2024/07/01/, 2024.

[4] F. Zhao, Z. Tian, and Y. Zeng, "Uncertainty Quantification in Gear Remaining Useful Life Prediction Through an Integrated Prognostics Method," IEEE Transactions on Reliability, vol. 62, no. 1, pp. 146-159, 2013.

[5] Y. Zhang, L. Fang, Z. Qi et al., "A Review of Remaining Useful Life Prediction Approaches for Mechanical Equipment," IEEE Sensors Journal, vol. 23, no. 24, pp. 29991-30006, 2023.

[6] H. Zhang, X. Xi, and R. Pan, "A two-stage data-driven approach to remaining useful life prediction via long short-term memory networks," Reliability Engineering and System Safety, vol. 237, 2023.

[7] S. Wang, H. Ma, Y. Zhang et al., "Remaining useful life prediction method of lithium-ion batteries is based on variational modal decomposition and deep learning integrated approach," Energy, vol. 282, 2023.

[8] J. Bi, X. Zhang, H. Yuan et al., "A Hybrid Prediction Method for Realistic Network Traffic With Temporal Convolutional Network and LSTM," IEEE Transactions on Automation Science and Engineering, vol. 19, no. 3, pp. 1869-1879, 2022.

[9] X. Li, C. Ye, B. Huang et al., "A Shortcut Enhanced LSTM-GCN Network for Multi-Sensor Based Human Motion Tracking," IEEE Transactions on Automation Science and Engineering, vol. 21, no. 4, pp. 5078-5087, 2024.

[10] Z. Wang, J. Cheng, H. Zheng et al., "Multistage Convolutional Autoencoder and BCM-LSTM Networks for RUL Prediction of Rolling Bearings," IEEE Transactions on Instrumentation and Measurement, vol. 72, pp. 1-13, 2023.

[11] Y. Wei, J. Jang-Jaccard, W. Xu et al., "LSTM-Autoencoder-Based Anomaly Detection for Indoor Air Quality Time-Series Data," IEEE Sensors Journal, vol. 23, no. 4, pp. 3787-3800, 2023.

[12] X. Yang, D. Chen, J. Huang et al., "Remaining Useful Life Prediction Under Multiple Operating Conditions Based on a Novel Dual-Layer Temporal Convolutional Network," IEEE Sensors Journal, vol. 25, no. 1, pp. 1900-1911, 2025.

[13] Z. Yang, Y. Wang, Y. Yang et al., "Remaining Useful Life Prediction Approach for Aviation Bearings Based on Multigenerator Generative Adversarial Network and CBAM," IEEE Transactions on Instrumentation and Measurement, vol. 74, pp. 1-9, 2025.

[14] W. Luo, W. Yang, J. He et al., "Fault Diagnosis Method Based on Two-Stage GAN for Data Imbalance," IEEE Sensors Journal, vol. 22, no. 22, pp. 21961-21973, 2022.

[15] Y. Zou, L. Yu, and K. He, "Forecasting crude oil risk: A multiscale bidirectional generative adversarial network based approach," Expert Systems with Applications, vol. 212, 2023.

[16] Y. Xiao, J. Yu, G. X. Xu et al., "An improved bidirectional generative adversarial network model for multivariate estimation of correlated and imbalanced tunnel construction parameters," JOURNAL OF ROCK MECHANICS AND GEOTECHNICAL ENGINEERING, vol. 15, no. 7, pp. 1797-1809, JUL, 2023.

[17] Q. Su, B. Tian, H. Wan et al., "Anomaly Detection Under Contaminated Data With Contamination-Immune Bidirectional GANs," IEEE Transactions on Knowledge and Data Engineering, vol. 36, no. 11, pp. 5605-5620, 2024.